Surface Innovations
Volume 3 Issue SI1
Dental implants coated with a durable and antibacterial film
Vogel *et al.*

ice | science

Pages 27–38 http://dx.doi.org/10.1680/si.14.00002
Research Article
Received 23/01/2014 Accepted 27/03/2014
Published online 30/03/2014
Keywords: antibacterial/biocompatibility/biomaterials/characterization/chemical vapor deposition/physical vapor deposition/plasma processing

ice Institution of Civil Engineers publishing

Dental implants coated with a durable and antibacterial film

Konstantin Vogel Dipl-Ing (FH)*
Adhesive Bonding Technology and Surfaces, Fraunhofer Institute for Manufacturing Technology and Advanced Materials, Bremen, Germany

Nina Westphal MSc
Adhesive Bonding Technology and Surfaces, Fraunhofer Institute for Manufacturing Technology and Advanced Materials, Bremen, Germany

Dirk Salz Dr
Adhesive Bonding Technology and Surfaces, Fraunhofer Institute for Manufacturing Technology and Advanced Materials, Bremen, Germany

Karsten Thiel Dr
Adhesive Bonding Technology and Surfaces, Fraunhofer Institute for Manufacturing Technology and Advanced Materials, Bremen, Germany

Linda Wittig MSc
Adhesive Bonding Technology and Surfaces, Fraunhofer Institute for Manufacturing Technology and Advanced Materials, Bremen, Germany

Lucio Colombi Ciacchi Prof Dr-Ing
Hybrid Materials Interfaces Group, Faculty of Production Engineering and Center for Environmental Research and Sustainable Technology, University of Bremen, Bremen, Germany

Ingo Grunwald Dr*
Adhesive Bonding Technology and Surfaces, Fraunhofer Institute for Manufacturing Technology and Advanced Materials, Bremen, Germany

Bacterial adhesion to the surface of implants in bone tissue may result in serious peri-implant diseases and cannot always be avoided by sterilization prior to implantation. For this reason, different strategies to confer the implant surfaces with intrinsic antibacterial properties are being developed. A major difficulty is that effective antibacterial materials may be detrimental to the adhesion of eukaryotic cells, and be poorly integrated into the host tissue. Here, we develop and characterize a composite coating material comprising silver nanoparticles deeply buried inside a matrix of plasma-polymerized hexamethyldisiloxane. Applied to titanium dental screws, the coating shows a good resistance against stresses from sterilization with β-irradiation and drilling into bone tissue. By varying the parameters of the plasma-depositing process, we are able to either induce or hinder the adhesion of epithelial cells. Through a fluorescence microscopy analysis, we demonstrate that the inclusion of silver nanoparticles in the polymer matrix does not influence the adhesion of fibroblasts and osteoblasts. However, the presence of silver in the coating layer results in dramatically reduced adhesion of *Escherichia coli* bacteria with respect to uncoated or silver-free coated surfaces.

1. Introduction

Biofilms on dental implant surfaces may lead to inflammatory lesions in the peri-implant mucosa.[1] Thus, osseointegration might be inhibited, eventually causing loss of surrounding bone material and at the worst total implant loss.[1] Several methods aiming to preclude the formation of bacterial films are currently being studied. This can involve a tuning of the surface topography[2] or surface chemistry,[3] but in any case, the performance of the implant in fulfilling its purpose as a function-replacing device must be preserved. This means that, even if bacteria are repelled, host cells are not to be harmed in order to guarantee optimal integration into the bone tissue. To this aim, biocompatible surfaces have been developed for instance via the inclusion of immobilized antimicrobial agents. Besides antibiotic drugs[4] or other metals,[5] silver has been in the focus of many studies because of its trusted antimicrobial performance and its well-accepted circulation in every day's life. Silver-coated implants have shown very promising results. For instance, in one case, a reduction of the infection rate from 47 to 7% has been observed *in vivo*.[6] However, it seems to be advisable to avoid overdoses and control the release of silver ions into the surrounding tissue in order to avoid the occurrence of unwanted toxic effects due to the contact of silver nanoparticles with eukaryotic cells.[7]

Several groups have addressed the technological problem of embedding silver nanoparticles into matrices.[8,9] The goal of this approach is to control the release of silver ions when the matrices are placed in contact with biological fluids. In particular, plasma-polymerized hexamethyldisiloxane (PP-HMDSO or, briefly, PP) was investigated as a coating material deposited on titanium dental implants.[10] Recently, a method for creating Ag/PP composites has been suggested as a promising route toward biomedical applications.[11] This is to be considered as a variation of a method developed early in our institution,[12] where silver nanoparticles were

***Corresponding author e-mail addresses:** konstantin.vogel@uni-bremen.de; ingo.grunwald@ifam.fraunhofer.de

embedded between two layers of PP by means of subsequent plasma polymerization and metal evaporation steps. The double PP/Ag/PP layer can be directly deposited on titanium implants, whose *in vivo* biocompatibility within soft tissues has been investigated in Ref. [13].

Building up on these previous results, in this article, we investigate the performances of a similar PP/Ag/PP-layered coating material (briefly, PP+Ag) toward the adhesion of bacteria and eukaryotic cells *in vitro*. In particular, besides HeLa cellular models, the adhesion behavior of fibroblasts and osteoblasts will be addressed. With respect to the original coating procedure,[12,13] physical vapor deposition is used instead of evaporation to deposit the silver nanoparticle layer. The advantage of the physical vapor deposition is a better control and reproducibility of the nanoparticle distribution and a lesser degree of nanoparticle agglomeration. We test the coating layer resistance to sterilization and implantation into bone tissue (Section 3.2), optimize the plasma deposition parameters to guarantee eukaryotic adhesion (Section 3.3) and check the successful bacterial deterrence of the coating in fluorescence microscopy images (Section 3.4).

2. Materials and methods

2.1 Plasma polymerization and layer formation

The plasma polymerization and deposition of silver nanoparticles are performed in the same plasma reactor chamber. A sample holder with rotating platforms is mounted inside a 125-liter vacuum chamber. The chamber comprises an electrode of rectangular shape and a silver target situated behind a shutter system. Gas inlets for the HMDSO precursor (Wacker, Munich, Germany), argon, oxygen and hydrogen (Linde AG, Pullach, Germany) and a pumping system are connected to the chamber walls. In this study, three different coating layers are investigated: (*a*) A 2000-nm-thick polymer coating without silver particles, which possesses cell-repelling properties (PP2000); (*b*) a 100-nm-thick coating without silver particles, which promotes eukaryotic adhesion (PP100) and (*c*) the same coating including silver nanoparticles to inhibit bacterial growth but not eukaryotic adhesion (PP100+Ag). The coating layers are produced as follows: After decreasing the chamber pressure below 10^{-4} mbar, HMDSO and oxygen are injected to a working pressure of 10^{-2} to 10^{-3} mbar. Applying a power of 160 W for 120 s, the plasma is ignited, and a 50-nm-thick polymer preconditioning layer is formed. The 2000-nm-thick coating is prepared at 120 W and oxygen to HMDSO gas flow ratio of 1:2. On top of the preconditioning layer, either the plasma polymerization is carried on until the desired thickness is reached (e.g. 100 nm for PP100), or an intermediate layer of silver nanoparticles is deposited by applying a power of 200 W for 60 s between the silver target and the chamber walls. With this procedure, we coat sand-blasted and etched titanium dental implant screws (11·5-mm length, 5·5-mm diameter) as well as titanium discs (10-mm diameter, 5-mm height), supplied by Nanolize GmbH (Hirschberg, Germany). The implant screws are investigated toward their sterilization resistance and mechanical durability, whereas the flat surfaces of the discs are used for cell culture and microscopy. PP100+Ag is deposited on carbon-coated copper grids for transmission electron microscopy (TEM) top view imaging. Small titanium cylinders (6-mm length, 3-mm diameter) are coated accordingly for a proliferation assay.

2.2 TEM-lamella preparation

To visualize the structure of the layer system, a thin lamella was first fabricated (50 nm) by means of focused ion (Ga^+) beam (FIB) preparation using a DualBeam – FEI Helios Nanolab 600 system (FEI, Hillsboro, USA). The resolution of the FIB is 5 nm at 30-kV accelerating voltage. For convenience, a smooth steel sample substrate is used. Before cutting, the whole sample surface is protected with a few micrometer-thick platinum patch deposited by chemical vapor deposition directly in the FIB. Subsequently, a lamella was cut out of the substrate, transferred to an Omniprobe TEM sample holder with an Omniprobe micromanipulator, thinned to electron transparency and finally polished.

2.3 Mechanical durability

To ensure the resistance of the layer system against stress from sterilization and screwing into bone tissue, dental implants are coated with PP100+Ag layers and sterilized using β-irradiation at 10 MeV and a dose of at least 25 kGy (BGS Beta-Gamma-Service GmbH & Co. KG, Bruchsal, Germany). Afterward, they are screwed into dead pig jawbone supplied by a local butcher and after explantation by breaking the bone further analyzed by Energy-dispersive X-ray analysis (EDX) using the FEI DualBeam system. Different sample areas have been investigated (measurements in triplicate). These steps are visualized in Figure 1.

2.4 Cell culture

The cell cultures utilized comprise immortalized mouse fibroblast L929 (DSMZ no: ACC 2, Braunschweig, Germany), immortalized human epithelial cell line HeLa (DSMZ no: ACC 57, Braunschweig, Germany) and human osteosarcoma cell line MG-63 (CLS no: 800125, Eppelheim, Germany). L929 and HeLa cells are cultured with RPMI 1640 with L-glutamine (Bio Whittaker Lonza, Verviers, Belgium), and MG-63 is cultured in Mc Coy's A medium with L-glutamine (Bio Whittaker Lonza, Verviers, Belgium). The media are supplemented with 10% fetal bovine serum (Biochrom, Berlin, Germany) and a final concentration of 100 U penicillin and 100 µg/ml streptomycin (Sigma-Aldrich, Steinheim Germany). Cells are grown at a desired density in cell culture flasks at 37°C in a humidified atmosphere of 5% carbon dioxide and subcultured twice a week. Titanium discs coated with PP2000, PP100 and PP100+Ag layers are placed into a 24-well plate and incubated with each cell line at a density of $7{\cdot}5 \times 10^4$ cells/well. The incubation of the cells is performed for 24 h at 37°C and 5% carbon dioxide under humidified atmosphere.

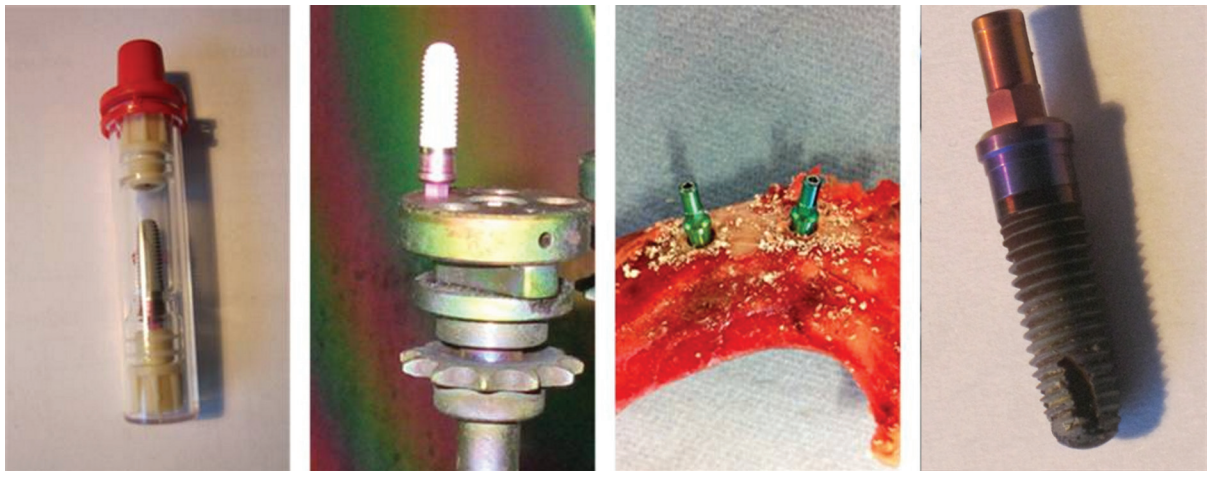

(a) (b) (c) (d)

Figure 1. Processing of the implant screw. The uncoated implant (a), β-irradiated while in the glass vessel, is placed onto a rotating sample holder at the center of the bifunctional PECVD/PVD reaction chamber (b) and screwed into pig jawbone after coating (c). The implant is recovered by breaking the bone to avoid stress from screwing out. After explantation (d), the implant shows spots of contamination in bone tissue (arrow). PECVD, plasma-enhanced chemical vapor deposition; PVD, physical vapor deposition

2.5 Cell microscopy

For evaluation of the cell attachment and morphological state, cells are visualized with fluorescence microscopy and scanning electron microscopy (SEM) images. A minimum of nine digital images have been acquired for each sample, and representative images are displayed in the picture reported in this article.

2.5.1 Fluorescence microscopy

After incubation, the L929 and MG-63 cells on PP100 and PP100+Ag, titanium discs are washed twice with phosphate-buffered saline (PBS) followed by fixation with 4% formaldehyde in PBS (Sigma-Aldrich, Steinheim, Germany) for 10 min. Samples are washed again twice with PBS, and cell membranes are permeabilized with ice cold acetone (Carl Roth, Karlsruhe, Germany) for 3 min. Following a repeated washing step, cells are incubated for 20 min in dark with the Alexa fluor 658 phalloidine solution at a concentration of 1:40 in PBS for staining F-actin. Cells are washed again, and the nuclei are counterstained with Hoechst 3334, two drops per milliliter (Life Technologies Corporation, Eugene, USA). At the end of the incubation period of 20 min, samples are washed, and cell adhesion is visualized using a fluorescence microscope (Axio Zeiss Imager A1 with AxioCam MRn, Jena, Germany). All procedures are performed at room temperature.

2.5.2 SEM

The fixation and washing steps for uncoated titanium discs and PP100+Ag as well as PP2000 are performed at room temperature and 130 rpm unless otherwise specified. All chemicals used are delivered from Sigma-Aldrich, Steinheim, Germany. Stock solution of 0·2 M sodium-cacodylate buffer is prepared, supplemented with 4% sucrose and pH adjusted to 7·4. Cells are washed twice with PBS for 2 min and fixed with 2% glutaraldehyde solution in 0·1 M sodium-cacodylate buffer for 30 min. Cells are washed with 0·1 M sodium-cacodylate buffer and dehydrated with an increasing ethanol gradient. Dehydration is performed dropwise with 30% ethanol followed by 50, 70 and two times with 100% for 2 min. Samples are submersed three times in 100% hexamethyldisilazane for 15 min and left to dry overnight in a vessel with a filter paper on top to avoid fast drying.

Samples are sputtered with gold, and SEM images are taken with the DualBeam – FEI Helios Nanolab 600 system. The resolution of the SEM is 0·9 nm at 15 kV and 1·4 nm at 1-kV accelerating voltage. The samples are coated with a thin gold layer to avoid charging. EDX is used for elemental analysis with an Oxford X-Max80-EDX detector and an energy resolution of 129 eV.

2.6 Antibacterial testing

2.6.1 Fluorescence imaging

The antimicrobial properties of the coated titanium samples are tested after exposure to Gram-negative *Escherichia coli* DH5α (DSMZ no: 4509, Braunschweig, Germany). *E. coli* is used here as a model Gram-negative bacterium, following previous studies concerning the antibacterial activity of silver nanoparticles (see Ref. [14]). For culturing, a fresh colony forming unit (cfu) of *E. coli* is scraped from an agar surface and inoculated into lysogeny broth (LB). The culture is grown overnight at 37°C under agitation at 250 rpm. After inoculation, the cell density is measured with ultraviolet–visible spectroscopy assuming that an optical density

(OD) value of 0·06 at 670 nm corresponds to 2×10^8 cells/ml (as determined in previous tests). The titanium samples are placed into a 24-well culture plate and covered with 1 ml of the bacterial suspension (*E. coli* in LB) with a density of 1×10^8 cells/ml[15–17] at 37°C without rotation for 90 min to achieve bacterial adherence. Subsequently, the media and floating cells are replaced against fresh media, and the incubation is continued for 24–72 h.[18] The coated titanium discs with adhered bacteria are washed two times with PBS and stained with SYTO 9 (green fluorescent) for live and intact cells and with propidium iodide (red fluorescent) for dead bacteria (LIVE/DEAD BacLight Bacterial Viability Kit, Invitrogen, USA). Triplicates of samples are analyzed with fluorescence microscopy (Zeiss Axio Imager M1, Carl Zeiss, Jena, Germany) to analyze the antimicrobial effect of the coated layers.

2.6.2 Proliferation assay

To investigate the bacterial proliferation on our coating film, we have followed a method adapted from Bechert *et al.*[19] with *E. coli* as the model organism. The small titanium cylinders are placed in a 96-microtiter plate, inoculated with 150 µl of a bacterial suspension (5 × 106 cfu/ml) and incubated under shaking at 250 rpm for 1 h at 37°C. The specimens are transferred into a fresh 96-microtiter plate. PBS of 200 µl are added, followed by 10 min of shaking at 250 rpm to wash off non-attached bacteria. Again, the specimens are transferred into a 96-microtiter plate already filled with 150 µl LB and incubated at 250 rpm for 18 h at 37°C. In this period, the attached cells can release daughter cells. Afterward, the specimens are removed from the wells, 100-µl LB media is added, and the bacterial growth is assessed over a period of 48 h. The growth is followed online at 37°C with a microplate reader (Mithras LB940, Berthold Technologies, Germany) by OD measurement at 620 nm every 30 min. Between the measurements, the plate is agitated to avoid settlement of the bacteria.

3. Results

3.1 Layer system structure

The coating layers are fabricated as described in Section 2 and imaged in cross-section and top view with TEM (Figure 2). Image (Figure 2(a)) clearly shows the layered system structure composed by silver particles (bright spots) embedded between two plasma polymer layers (dark areas) on top of the metal substrate (gray area at the bottom). Nanoparticle size, morphology and repartition can be seen in the top view image of a carbon-coated copper grid (Figure 2(b)).

3.2 Mechanical durability

The resistance of the PP100+Ag layer system toward sterilization and implantation into bone tissue is investigated by sterilization with β-irradiation followed by screwing into dead pig jawbone. Afterward, the titanium screws are explanted by breaking the bone structure and imaged with SEM. Contaminations from bone tissue induced by the drilling process can clearly be seen with naked eye between the ridges of the screw thread (Figure 1(d)). However, portions of the implant surface free from contaminations can be found on SEM analysis (Figure 3, arrow). This enables us to perform an EDX analysis of the surface composition after explantation without the need of any additional cleaning procedure. Besides an abundance of titanium, the EDX analysis shows the presence of silicon and an silver content of 1·8%. In comparison, on the not implanted but coated surface, silicon and silver are present in similar quantity. This indicates that the sterilization and implantation do not cause detachment or serious damage of the PP100+Ag coating layer.

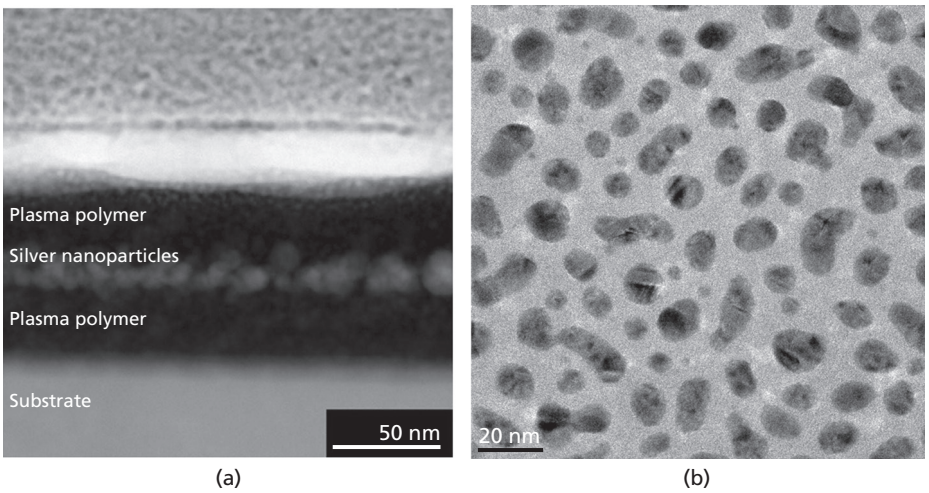

(a) (b)

Figure 2. TEM analysis of the PP100+Ag sandwich coating: (a) The layer system comprises an underlying matrix of plasma-polymerized HMDSO, sputtered silver nanoparticles and a second coating of plasma-polymerized HMDSO. The embedded nanoparticles are immobilized, but when immersed in media, silver ions are able to diffuse to the surface. (b) The top view image visualizes characteristics of the single particles. HMDSO, hexamethyldisiloxane; TEM, transmission electron microscopy

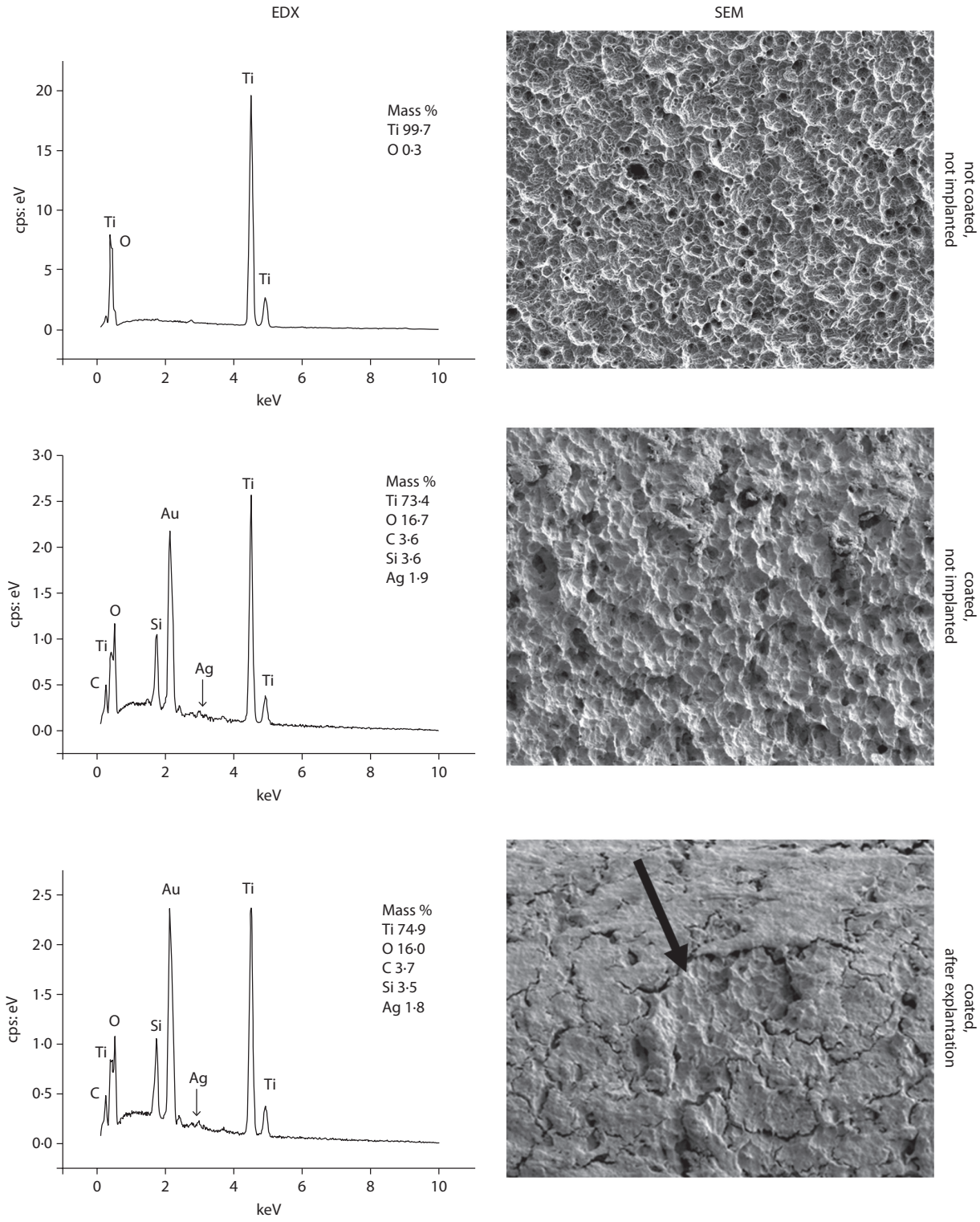

Figure 3. EDX analysis (left) and SEM images (right) of sterilized screws that were uncoated, PP100+Ag-coated before implantation and PP100+Ag-coated after explantation. The EDX analysis clearly shows, besides the abundance of titanium, the presence of silver after explantation. Contaminations of bone material can be seen on the explanted sample (bottom right). Nevertheless, contamination-free spots (arrow) allow for EDX measurements. EDX, energy-dispersive X-ray; SEM, scanning electron microscopy

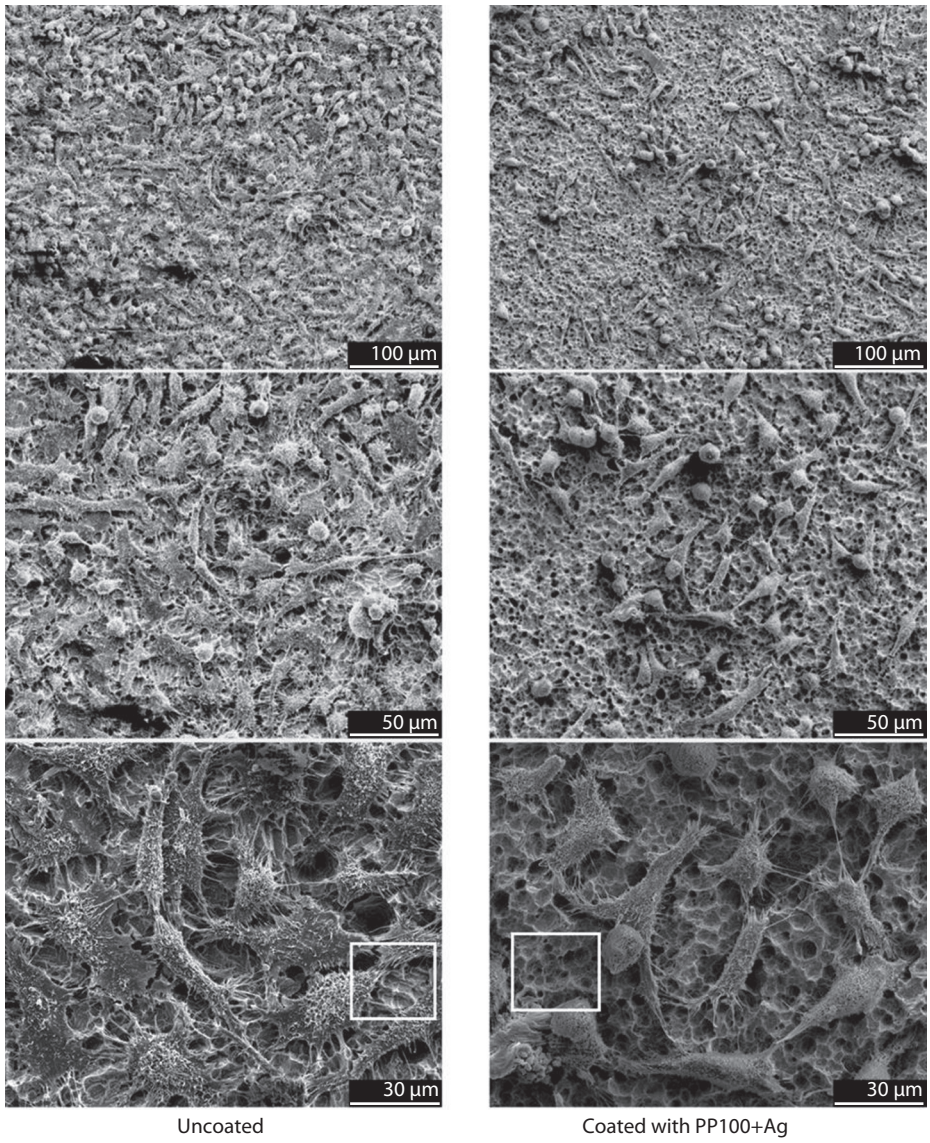

Figure 4. Exemplary SEM images of HeLa cells on uncoated and PP100+Ag-coated titanium surfaces. Titanium discs are incubated for 24 h at RT together with a suspension of 75 000 HeLa cells/ml and subsequently imaged by SEM. Left: Uncoated titanium surface; Right: titanium surface coated with the PP100+Ag layer. SEM, scanning electron microscopy; RT, room temperature

3.3 Eukaryotic cell adhesion

Figure 4 shows HeLa cells on uncoated and PP100+Ag-coated titanium discs after 24 h of incubation, at three different magnifications. The uncoated sample is densely covered with cells forming a tight network of cellular interconnections clearly visible at high magnification. The coated sample also shows attached cells, however, in a lower number. Cellular interconnections are again visible in the magnified pictures. The cell morphologies are not noticeably affected by the presence of the PP100+Ag coating. A closer inspection of surface areas not covered with cells (white rectangles in Figure 4) reveals that the pristine surface topography of the sand-blasted titanium discs is almost perfectly preserved after coating with the thin PP100+Ag layer.

In contrast, both the morphology and the cell adhesion properties are changed dramatically after coating the titanium surface with the PP2000 layer. This is shown in Figure 5, where we present SEM images of titanium discs that were partially masked during the coating procedure, resulting in a sharp interface between uncoated and PP2000-coated surfaces. The bare surface presents sharp edges and ridges resulting from sand blasting and etching. The coated surface still presents holes and more exposed spots, but with rather smooth transitions between one and the next spot. The cellular response to the two surfaces appears also to be markedly different. Compared with the bare titanium surface, only very few and less spread cells are able to adhere to the surface coated with the thick plasma polymer layer (Figure 5).

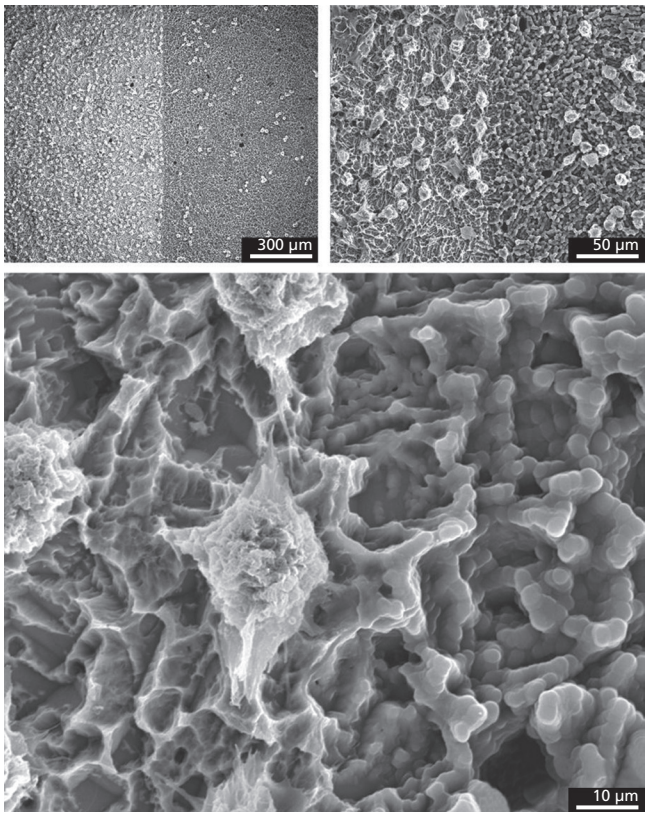

Figure 5. SEM images of HeLa cells on a titanium surface partially coated with PP2000 layer. The three different magnifications show a large degree of cellular adhesion on the uncoated sample part (left) and a very low number of cells on the coated part (right). Visible is also the change of surface topography induced by the plasma–polymer deposition. SEM, scanning electron microscopy

The response of fibroblasts and osteoblasts to the thinner coatings (PP100 and PP100+Ag) is visualized in the fluorescence microscopy images in Figure 6. After 24 h of incubation on the surfaces, the fibroblasts appear in roughly circular shapes, whereas the osteoblasts are more prominently spread and interconnected. Interestingly, both the amount of adhered cells and their degree of spreading are slightly affected by the underlying surface coatings. In particular, also the inclusion of silver nanoparticles in the plasma polymer layer does not seem to have a detrimental effect on the cellular behavior according to our investigation. We found these data to be reproducible in our laboratories at different times, with different stocks of chemicals, different stocks of cells and different stocks of substrates.

3.4 Antibacterial activity

The antibacterial activity of the PP100+Ag layer against *E. coli* is analyzed both using a proliferation assay and with fluorescence imaging of coated and uncoated titanium discs (Figure 7). For the uncoated and PP100-coated samples, a similar extent of bacterial proliferation is detected, whereas the PP100+Ag film effectively inhibits bacterial proliferation. For the fluorescence analysis, the discs are incubated in bacterial suspensions for 3 d and imaged after 72 h. The uncoated titanium samples show a homogeneous distribution of densely packed bacterial cells. The sample coated with PP100 presents a lower amount of adhered living bacteria. Much less living bacteria are found on the sample coated with PP100+Ag after 72 h of incubation. These results prove that the inclusion of silver nanoparticles into the plasma polymer effectively prevents the adhesion of bacteria on the coated titanium surface.

4. Discussion

The motivation of this study was the development of a coating for dental implants capable to give human cells a competitive edge over bacteria within the 'race to the surface'[20] after the implantation process. Our approach aimed to coat complex structures (such as screws) with an antibacterial layer not diminishing the desired biocompatible properties of titanium. Furthermore, the coating had to sustain chemical and mechanical stresses involved in the sterilization and the implantation processes, respectively.

All of these goals have been reached with the PP100+Ag layer system presented in this study and imaged in Figure 2. A similar composite system with silver nanoparticles embedded in a plasma-polymerized HMDSO matrix has been proposed, for example, by Saulou *et al.*[21] However, in that study, silver was sputtered simultaneously with plasma polymerization of HMDSO leading to distribution of silver across the whole matrix. In this study, the introduction of a conditioning layer of pure PP-HMDSO increases the adhesion to the metal substrate and prevents the risks of corrosion and abrasion induced by substrate/nanoparticle contacts. Moreover, confining the silver nanoparticles to a thin layer buried inside the polymer matrix avoids their direct exposure to the physiological tissues, thus reducing the potential toxicity of the layer toward eukaryotic cells.[22] Importantly, the antibacterial activity, arising from the dissolution of Ag^+ ions,[13] is not impaired given the water permeability of the PP-HMDSO film.[21] Saulou *et al.* showed the release of Ag^+ ions into deionized water from silver nanoparticles, which had been embedded in a plasma polymer matrix deposited from HMDSO.[21] It can be assumed that Ag^+ ions are formed when water enters the matrix and that the plasma polymer matrix is permeable to the ions. This is in line with work by Alt *et al.*, who embedded silver nanoparticles in a matrix of HMDSO.[12] They investigated the proliferation of *Staphylococcus epidermis* for 36 h on coated and uncoated substrates and emphasized the high porosity of the HMDSO matrix.

An important feature of our thin-film coating procedure, resulting in a coating thickness of the order of 100 nm or lower, is that the submicrometer roughness of the titanium surface, as achieved by sand-blasting and etching, is preserved on plasma coating (see for instance Figure 4). A sufficiently rough surface is

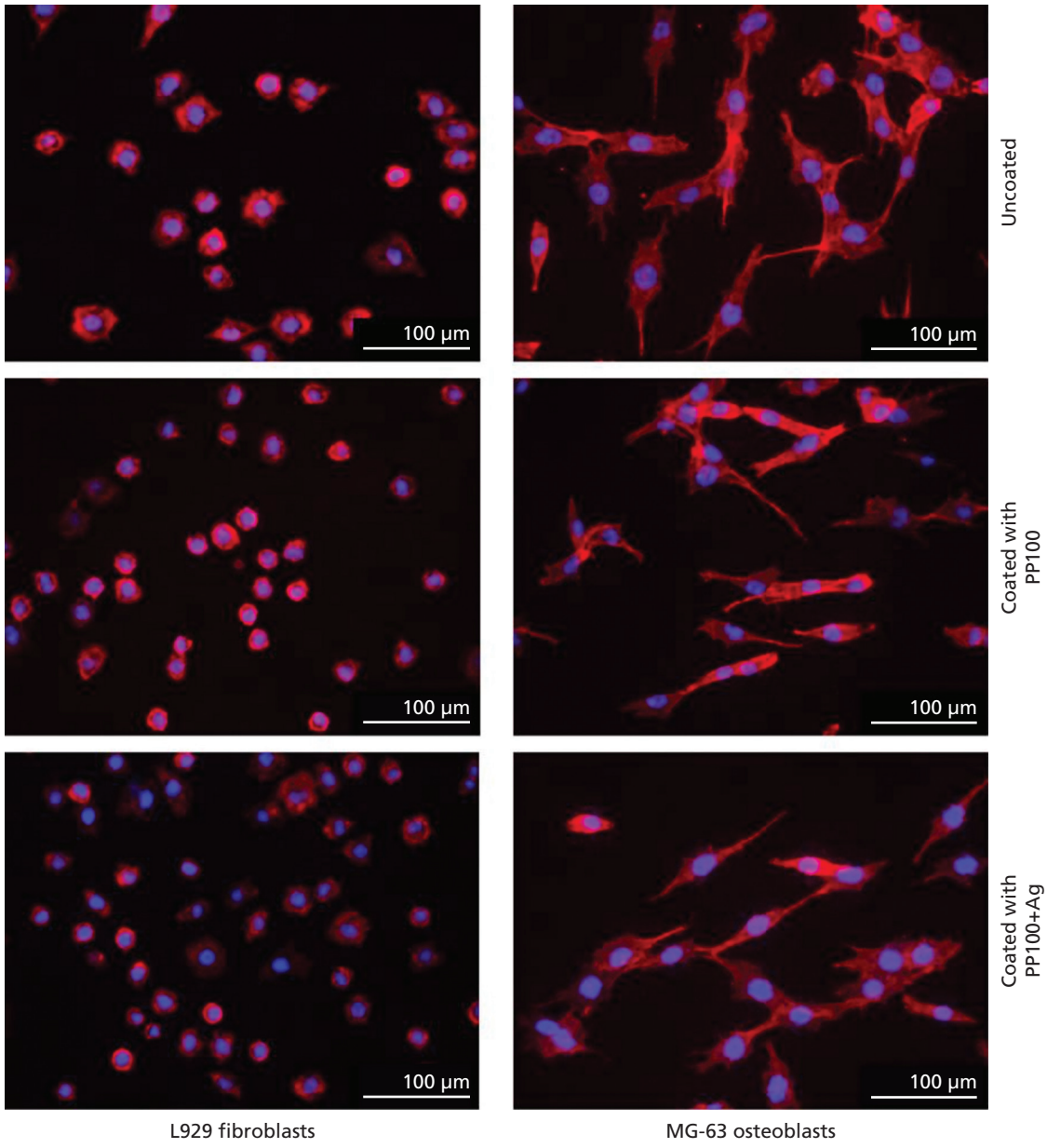

Figure 6. Fluorescence microscopy images of L929 fibroblasts and MG-63 osteoblasts on titanium surfaces uncoated, coated with PP100 and coated with PP100+Ag, after 24 h of incubation

desired to facilitate the adhesion of bone cells and results in an efficient osseointegration of the implant. Moreover, the chemical durability of the layer and its mechanical resistance are such that standard sterilization and implantation procedures do not lead to delamination or abrasion of the active coating, as demonstrated in Figure 3. After β-irradiation, implantation and subsequent explantation, silver could still be detected on the implant's surface, suggesting that antimicrobial activity might be expected under realistic usage conditions.

4.1 Eukaryotic cell–surface interaction

Since dental implants need to be well integrated in the bone tissue to fulfill their load-bearing function, cellular adhesion on the coated implant is highly desired and is indeed preserved by our PP100+Ag coating (Figures 4 and 6). Cell adhesion is controlled both by surface topography[23] and surface chemistry. As mentioned above, the thickness of our PP100 coatings is low enough not to change the surface topography. Given that the cellular adhesion is diminished only little with respect to uncoated titanium samples,

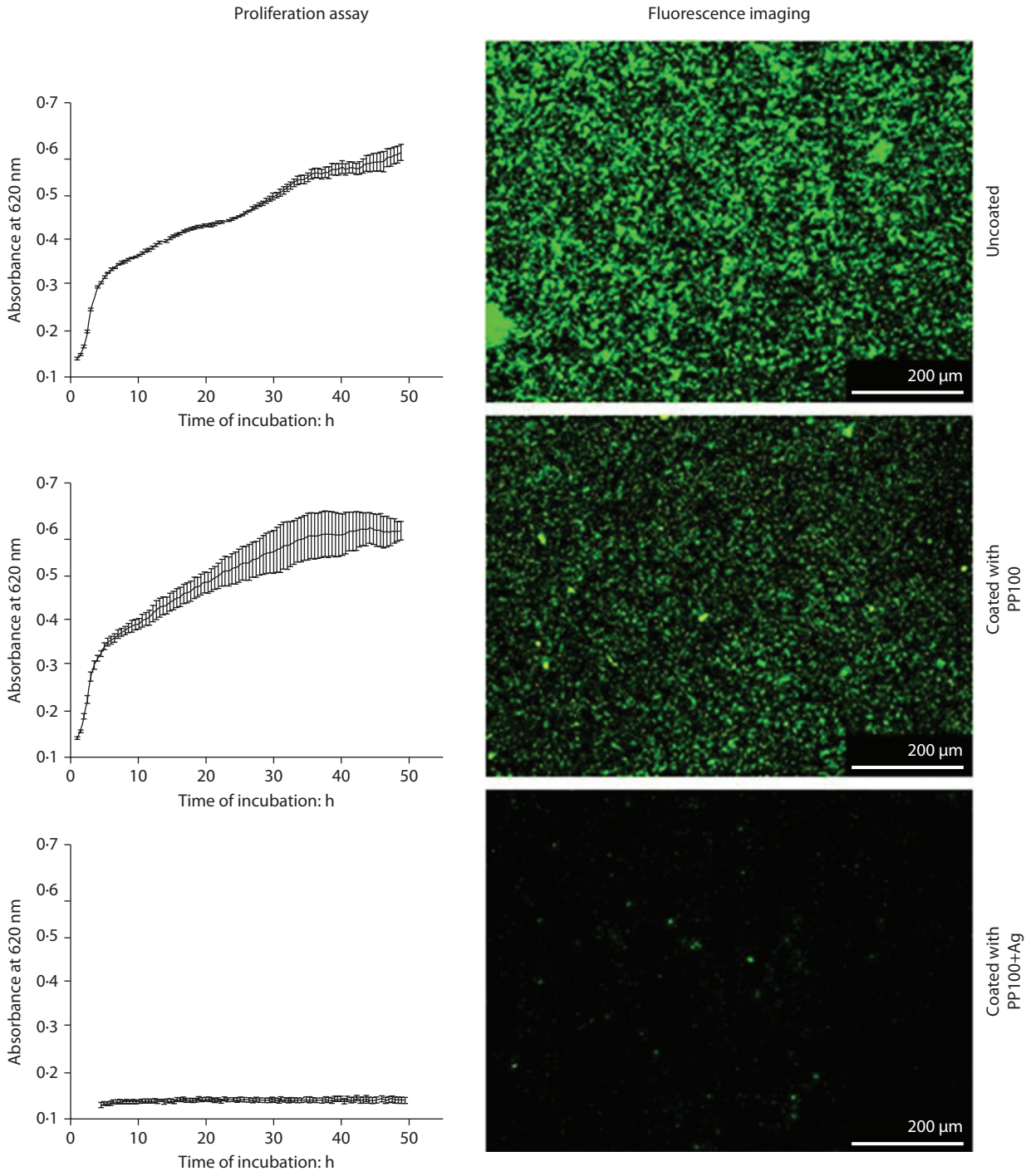

Figure 7. Growth curves (left) and fluorescence microscopy images (right) of *Escherichia coli* cultured on uncoated, PP100-coated and PP100+Ag-coated titanium. Proliferation is visible on uncoated and PP100 surfaces, whereas no proliferation is detected on PP100+Ag. The images show vital bacterial cells on the three different surfaces

we must conclude that the hydrophilicity of the film is high enough to ensure a good degree of eukaryotic cell adhesion. Importantly, the adhesion is not affected by the presence of silver nanoparticles in the coating, probably because the particles themselves are buried deep inside the matrix. In contrast, a hydrogel with a homogeneous distribution of silver nanoparticles developed by Fullenkamp *et al.* via a wet chemical process[24] presented good antibacterial activity but poor mammalian cell adhesion properties.

Different is the case for the PP2000 coating, which visibly alters the surface topography. In this case, the adhesion and the spreading of HeLa cells is markedly reduced (Figure 5). Potentially, this kind of plasma coating can be of advantage in any application where cell adhesion needs to be avoided, for instance in the case of removable implants where an overgrown of tissue on their surfaces is detrimental.[25]

Fibroblasts and osteoblasts also adhere to the implant surface irrespective of the presence of the PP-HMDSO coating, with or without embedded silver nanoparticles (Figure 6). Compared to the MG-63 osteoblasts, the L929 fibroblasts spread to a minor extent over the surface, which can be taken as an indication of reduced adhesion dynamics[26] and possibly also of lower proliferation rate.[27] However, since the cellular spreading and proliferation depend strongly on the specific cell line[28] as well as on the surface topography,[29] investigations of several cell lines and in particular of primary cells should be performed before reaching a firm conclusion about the cell-specific response of our coating material.

4.2 Antibacterial activity

Silver nanoparticles are known to act as an antibacterial agent via the dissolution of Ag^+ ions.[13] In our PP100+Ag system, although the nanoparticles are not directly exposed to the outer coating's surface, dissolution and diffusion of silver ions out of the highly porous and water-permeable PP-HMDSO layer is readily possible.[21] Indeed, *E. coli* bacteria are not found to grow on the silver-containing layer. Compared with uncoated titanium surfaces, where a high number of bacteria have been detected by fluorescence spectroscopy, the presence of a PP-HMDSO layer already leads to a diminished number of adhered bacteria, probably due to reduced adhesion capability on the polymer matrix (Figure 7). The effect of the inclusion of silver nanoparticles in the matrix is dramatic, and very limited bacterial adhesion is observed both after 24 h and after 72 h of incubation in *E. coli* suspensions.

Interestingly, no dead bacteria could be detected by means of specific fluorescence labeling. This may suggest that the PP100+Ag coating effectively reduces the initial adhesion of bacteria from the suspension. Moreover, the proliferation of the few adhering bacteria, which occurs rapidly on uncoated titanium surfaces (see Figure 7), might be inhibited by the release of silver ions from the underlying coating layer. In fact, Ag^+ is known to interfere in the respiratory chain of *E. coli* and to stop the DNA replication, which is necessary for the reproduction of cells.[30] Alt *et al.* used the same proliferation test for bone cement doped with silver nanoparticles[31] and succeeded in inhibiting bacterial growth, even for bacterial strains resistant to other antibiotics such as methicillin.

Similar antibacterial effects were observed for instance on silver-loaded titanium dioxide nanotubes by Zhao *et al.*,[32] who stressed the importance of achieving long-lasting antibacterial surface properties. This issue motivates, in particular, investigations aiming at an optimization of our PP-HMDSO+Ag coating regarding the release kinetics of Ag^+ ions. Parameters that are likely to influence the kinetics of ion release are, for instance, the absolute amount against the size distribution of the silver nanoparticles, or the porosity and thickness of the polymer matrix embedding the nanoparticles. The optimization should be performed under the constraint of the highest silver amount compatible with eukaryotic survival. These themes shall be addressed in future works. In particular, the highest silver amount compatible with eukaryotic cells should be assessed using well-established cytotoxicity tests on primary cells.

5. Conclusion

In conclusion, we have presented the successful development of an enduring Ag/HMDSO composite coating material for metal implant surfaces possessing antibacterial activity while, at the same time, preserving good adhesion properties for eukaryotic cells. The material can be easily applied, by means of plasma coating, to implants with complex morphologies such as sand-blasted and etched titanium dental screws, and is able to resist stresses due to sterilization and implantation. Key to the specific coating functionality is the physical separation of the silver nanoparticles from adhering eukaryotic cells via a thin layer of plasma-polymerized HMDSO. The porosity and hydrophilicity of the coating, however, allow Ag^+ ions to be gradually released into the physiological fluids, hindering bacterial adhesion and proliferation. All steps of the coating process can be integrated in industrial production lines, thus in principle enabling a commercialization and wide distribution of the coating in the biomedical implant sector.

Acknowledgements

The authors thank the German Federal Ministry of Education and Research for funding of this work (BMBF, funding number 13N11141). LCC acknowledges funding from the EU-FP7-NMP grant 229205 ADGLASS. The authors are obliged to Neeti Sudumbrekar and Uwe Specht for technical assistance, to Andreas Witt and the BioGate AG for providing us with titanium samples and are also grateful to Ralph Wilken for his encouraging efforts.

REFERENCES

1. Berglundh, T.; Lindhe, J.; Lang, N. P. Peri-implant mucositis and peri-implantitis. In *Clinical Periodontology and Implant Dentistry*, 5th edn. (Lindhe, J.; Lang, N. P.; Karring, T. (eds.)). Oxford: Blackwell Munksgaard, 2008, 532.
2. Le Guehennec, L.; Soueidan, A.; Layrolle, P.; Amouriq, Y. Surface treatments of titanium dental implants for rapid osseointegration. *Dental Materials* **2007**, *23*(7), 844–854.
3. Thevenot, P.; Hu, W.; Tang, L. Surface chemistry influences implant biocompatibility. *Current Topics in Medicinal Chemistry* **2008**, *8*(4), 270–280.

4. Stigter, M.; Bezemer, J.; de Groot, K.; Layrolle, P. Incorporation of different antibiotics into carbonated hydroxyapatite coatings on titanium implants, release and antibiotic efficacy. *Journal of Controlled Release* **2004**, *99*(1), 127–137.
5. Kim, T. N.; Feng, Q. L.; Kim, J. O.; Wu, J.; Wang, H.; Chen, G. C.; Cui, F. Z. Antimicrobial effects of metal ions (Ag^{+}, Cu^{2+}, Zn^{2+}) in hydroxyapatite. *Journal of Materials Science: Materials in Medicine* **1998**, *9*(3), 129–134.
6. Gosheger, G.; Hardes, J.; Ahrens, H.; Streitburger, A.; Buerger, H.; Erren, M.; Gunsel, A.; Kemper, F. H.; Winkelmann, W.; Von Eiff, C. Silver-coated megaendoprostheses in a rabbit model – an analysis of the infection rate and toxicological side effects. *Biomaterials* **2004**, *25*(24), 5547–5556.
7. AshaRani, P. V.; Mun, G. L. K.; Hande, M. P.; Valiyaveettil, S. Cytotoxicity and genotoxicity of silver nanoparticles in human cells. *ACS Nano* **2009**, *3*(2), 279–290.
8. Yang, L.; Chen, Q.; Sang, L.; Wang, Z.; Liu, Z. The role of monomer size and facet of crystal silver nanoparticles obtained by plasma technology. *Surface and Coatings Technology* **2013**, *228*(Suppl. 1), 28–32.
9. Sotiriou, G. A.; Teleki, A.; Camenzind, A.; Krumeich, F.; Meyer, A.; Panke, S.; Pratsinisa, S. E. Nanosilver on nanostructured silica: antibacterial activity and Ag surface area. *Chemical Engineering Journal* **2011**, *170*(2–3), 547–554.
10. Hayakawa, T.; Yoshinari, M.; Nemoto, K. Characterization and protein-adsorption behavior of deposited organic film onto titanium by plasma polymerization with hexamethyldisiloxane. *Biomaterials* **2004**, *25*(1), 119–127.
11. Peter, T.; Rehders, S.; Schuermann, U.; Strunskus, T.; Zaporojtchenko, V.; Faupel, F. High rate deposition system for metal-cluster/$SiO_xC_yH_z$-polymer nanocomposite films. *Journal of Nanoparticle Research* **2013**, *15*(6), 1710.
12. Alt, V.; Wagener, M.; Salz, D.; Bechert, T.; Steinruecke, P.; Schnettler, R. Plasma polymer – high porosity silver composite coating for infection prophylaxis in intramedullary nailing. *Practice of Intramedullary Locked Nails* **2006**, 297–303.
13. Khalilpour, P.; Lampe, K.; Wagener, M.; Stigler, B.; Heiss, C.; Ullrich, M. S.; Domann, E.; Schnettler, R.; Alt, V. Ag/SiO_xC_y plasma polymer coating for antimicrobial protection of fracture fixation devices. *Journal of Biomedical Materials Research Part B: Applied Biomaterials* **2010**, *94B*(1), 196–202.
14. Sondi, I.; Salopek-Sondi, B. Silver nanoparticles as antimicrobial agent: a case study on *E. coli* as as model for Gram-negative bacteria. *Journal of Colloid and Interface Science* **2004**, *275*, 177–182.
15. Prosser, B. L.; Taylor, D.; Dix, B. A.; Cleeland, R. Method of evaluating effects of antibiotics on bacterial biofilm. *Antimicrobial Agents and Chemotherapy* **1987**, *31*(10), 1502–1506.
16. Vesterlund, S.; Paltta, J.; Karp, M.; Ouwehand, A. C. Measurements of bacterial adhesion – in vitro evaluation of different methods. *Journal of Microbiological Methods* **2005**, *60*(2), 225–233.
17. Peeters, E.; Nelis, H. J.; Coenye, T. Comparison of multiple methods for quantification of microbial biofilms grown in microtiter plates. *Journal of Microbiological Methods* **2008**, *72*(2), 157–165.
18. Purschke, F. G. *Phaenotypische und molekularbiologische Untersuchungen der Interaktionen in gemischten Biofilmen*. PhD thesis, University of Stuttgart, Stuttgart, Germany, 2012.
19. Bechert, T.; Steinrucke, P.; Guggenbichler, J. P. A new method for screening anti-infective biomaterials. *Nature Medicine* **2000**, *6*, 1053–1056.
20. Subbiahdoss, G.; Kuijer, R.; Grijpma, D. W.; van der Mei, H. C.; Busscher, H. J. Microbial biofilm growth vs. tissue integration: "The race for the surface" experimentally studied. *Acta Biomaterialia* **2009**, *5*(5), 1399–1404.
21. Saulou, C.; Despax, B.; Raynaud, P.; Zanna, S.; Marcus, P.; Mercier-Bonin, M. Plasma deposition of organosilicon polymer films with embedded nanosilver for prevention of microbial adhesion. *Applied Surface Science* **2009**, *256*(Suppl. 3), 35–39.
22. Harris, L. G.; Richards, R. G. Staphylococci and implant surfaces: a review. *Injury* **2006**, *37*(Suppl. 2), 3–14.
23. Curtis, A.; Wilkinson, C. Topographical control of cells. *Biomaterials* **1997**, *18*(24), 1573–1583.
24. Fullenkamp, D. E.; Rivera, J. G.; Gong, Y-K.; Lau, K. H. A.; He, L.; Varshney, R.; Messersmith, P. B. Mussel-inspired silver-releasing antibacterial hydrogels. *Biomaterials* **2012**, *33*(15), 3783–3791.
25. Doi, K.; Oue, H.; Morita, K.; Kajihara, S.; Kubo, T.; Koretake, K.; Perrotti, V.; Iezzi, G.; Piattelli, A.; Akagawa, Y. Development of implant/interconnected porous hydroxyapatite complex as new concept graft material. *PLoS One* **2012**, *7*(11), e49051 11.
26. He, T.; Shi, Z. L.; Fang, N.; Neoh, K. G.; Kang, E. T.; Chan, V. The effect of adhesive ligands on bacterial and fibroblast adhesions to surfaces. *Biomaterials* **2009**, *30*(3), 317–326.
27. Schneider, G.; Burridge, K. Formation of focal adhesions by osteoblasts adhering to different substrata. *Experimental Cell Research* **1994**, *214*(1), 264–269.
28. Hunter, A.; Archer, C. W.; Walker, P. S.; Blunn, G. W. Attachment and proliferation of osteoblasts and fibroblasts on biomaterials for orthopaedic use. *Biomaterials* **1995**, *16*(4), 16.
29. Bellows, C. G.; Aubin, J. E.; Heersche, J. N. M.; Antosz, M. E. Mineralized bone nodules formed in vitro from enzymatically released rat calvaria cell populations. *Calcified Tissue International* **1986**, *38*(3), 143–154.

30. Secinti, K. D.; Oezalp, H.; Attar, A.; Sargon, M. F. Nanoparticle silver ion coatings inhibit biofilm formation on titanium implants. *Journal of Clinical Neuroscience* **2011**, *18*(3), 391–395.
31. Alt, V.; Bechert, T.; Steinruecke, P.; Wagener, M.; Seidel, P.; Dingeldein, E.; Domann, E.; Schnettler, R. An in vitro assessment of the antibacterial properties and cytotoxicity of nanoparticulate silver bone cement. *Biomaterials* **2004**, *25*, 4383–4391.
32. Zhao, L.; Wang, H.; Huo, K.; Cui, L.; Zhang, W.; Ni, H.; Zhang, Y.; Wu, Z.; Chu, P. K. Antibacterial nano-structured titania coating incorporated with silver nanoparticles. *Biomaterials* **2011**, *32*(24), 5706–5716.